

# CALIFORNIA INSTITUTE OF TECHNOLOGY

## EARTHQUAKE ENGINEERING RESEARCH LABORATORY

### RESULTS OF MILLIKAN LIBRARY FORCED VIBRATION TESTING

BY

S C BRADFORD, J F CLINTON, J FAVELA, T H HEATON

REPORT No. EERL 2004-03

PASADENA, CALIFORNIA

FEBRUARY 2004



## **ACKNOWLEDGMENTS**

The authors would like to acknowledge Arnie Acosta for data triggering and retrieval, and thank him for his support. We thank Caltech's Structural Monitoring Group for their input during this project, and we also thank the Southern California Earthquake Center and the Portable Broadband Instrumentation Center at the University of California Santa Barbara for the loan of the portable instrument. We acknowledge the SCEDC for the MIK data.

A report on research supported by the  
CALIFORNIA INSTITUTE OF TECHNOLOGY

## **ABSTRACT**

This report documents an investigation into the dynamic properties of Millikan Library under forced excitation. On July 10, 2002, we performed frequency sweeps from 1 Hz to 9.7 Hz in both the East-West (E-W) and North-South (N-S) directions using a roof level vibration generator. Natural frequencies were identified at 1.14 Hz (E-W fundamental mode), 1.67 Hz (N-S fundamental mode), 2.38 Hz (Torsional fundamental mode), 4.93 Hz (1<sup>st</sup> E-W overtone), 6.57 Hz (1<sup>st</sup> Torsional overtone), 7.22 Hz (1<sup>st</sup> N-S overtone), and at 7.83 Hz (2<sup>nd</sup> E-W overtone). The damping was estimated at 2.28% for the fundamental E-W mode and 2.39% for the N-S fundamental mode. On August 28, 2002, a modal analysis of each natural frequency was performed using the dense instrumentation network located in the building. For both the E-W and N-S fundamental modes, we observe a nearly linear increase in displacement with height, except at the ground floor which appears to act as a hinge. We observed little basement movement for the E-W mode, while in the N-S mode 30% of the roof displacement was due to basement rocking and translation. Both the E-W and N-S fundamental modes are best modeled by the first mode of a theoretical bending beam. The higher modes are more complex and not well represented by a simple structural system.

**TABLE OF CONTENTS**

**1 INTRODUCTION 1**

**2 MILLIKAN LIBRARY 2**

2.1 Historical Information . . . . . 2

2.2 Millikan Library Shaker . . . . . 6

2.3 Millikan Library Instrumentation . . . . . 8

**3 FREQUENCY SWEEP 9**

**4 MODESHAPE TESTING 12**

4.1 Procedure and Data Reduction . . . . . 12

4.2 Fundamental Modes . . . . . 14

4.3 Higher Order Modes . . . . . 19

4.4 Modeshapes Summary . . . . . 24

**REFERENCES 28**

**A THEORETICAL BEAM BEHAVIOR 29**

**B HISTORICAL SUMMARY OF MILLIKAN LIBRARY STUDIES 32**

# 1 INTRODUCTION

This report documents the forced vibration testing of the Robert A. Millikan Memorial Library located on the California Institute of Technology campus. It also provides a historical backdrop to put our results in perspective.

During and immediately after the construction of the library in the late 1960s, numerous dynamic analyses were performed (Kuroiwa, 1967; Foutch et al, 1975; Trifunac, 1972; Teledyne-Geotech-West, 1972). In these analyses, fundamental modes and damping parameters were identified for the library, and higher order modes were suggested, but not investigated. It has been established that the fundamental frequencies of the library vary during strong motion (Luco et al, 1986; Clinton et al, 2003). Some drift in the long-term behavior of the building has also been observed in compiled reports of modal analysis from the CE180 class offered every year at Caltech (Clinton, 2004).

The temporal evolution of the building's dynamic behavior, as well as the much improved density and quality of instrumentation, led to an interest in a complete dynamic investigation into the properties of the system. Our experiments were designed to provide an updated account of the fundamental modes, and to identify and explore the higher order modes and modeshapes. A better understanding of the dynamic behavior of the Millikan Library will aid in the increased research being performed on the building, and provide a better understanding of the data currently being recorded by the instruments in the library.

An initial test was performed on July 10, 2002, for which we performed a full frequency sweep of the building (from 9.7Hz, the limit of the shaker, to 1Hz), in both the E-W and N-S directions. Frequencies of interest were explored in more detail, with a finer frequency spacing and different weight configurations, during a second test on August 28, 2002.



Figure 1. Robert A. Millikan Memorial Library: View from the Northeast. The two dark colored walls in the foreground comprise the East shear wall.

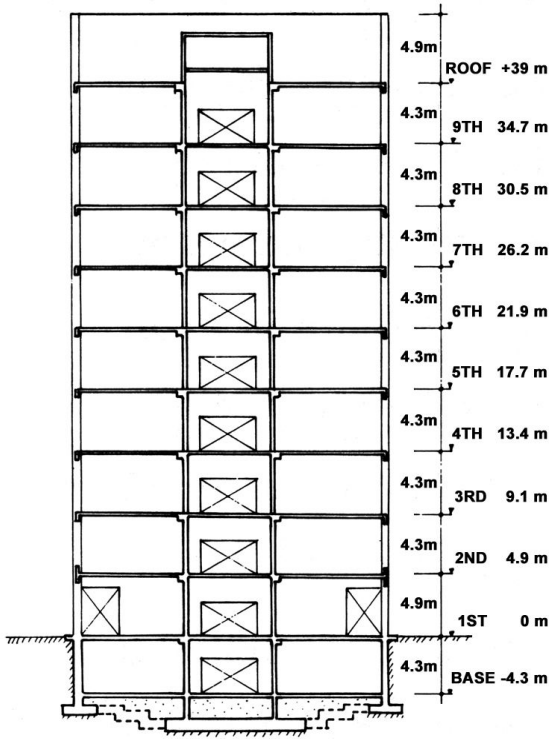
## **2 MILLIKAN LIBRARY**

The Millikan Library (Figure 1) is a nine-story reinforced concrete building, approximately 44m tall, and 21m by 23m in plan. Figure 2 shows plan views of the foundation and a typical floor, as well as cross-section views of the foundation and a N-S cross-section.

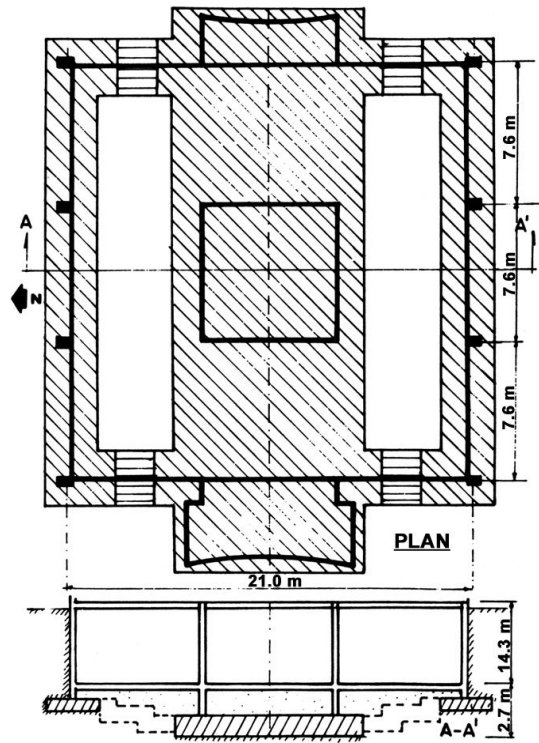
The building has concrete moment frames in both the E-W and N-S directions. In addition, there are shear walls on the East and West sides of the building that provide most of the stiffness in the N-S direction. Shear walls in the central core provide added stiffness in both directions. More detailed descriptions of the structural system may be found in Kuroiwa (1967), Foutch (1976), Luco et al. (1986), Favela (2003) and Clinton (2004).

### **2.1 Historical Information**

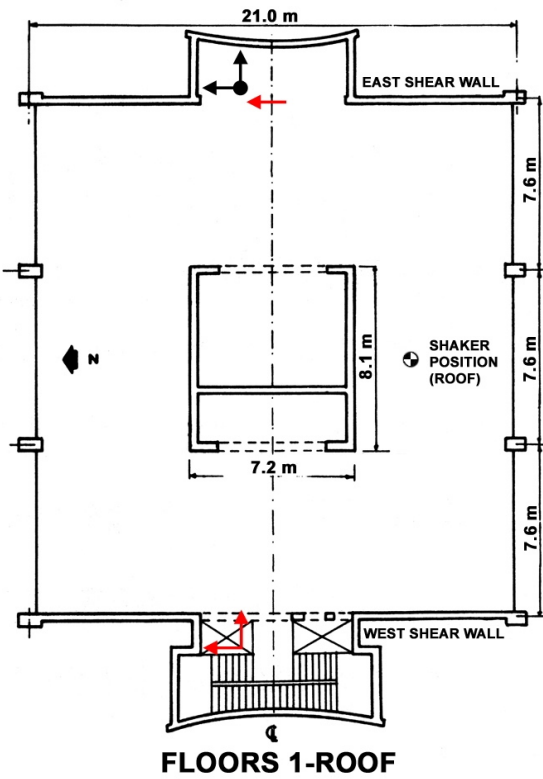
The Millikan Library has been extensively monitored and instrumented since its completion in 1966 (Kuroiwa, 1967; Trifunac, 1972; Foutch, 1976; Luco et al, 1986; Chopra, 1995). Clinton et al. (2003)



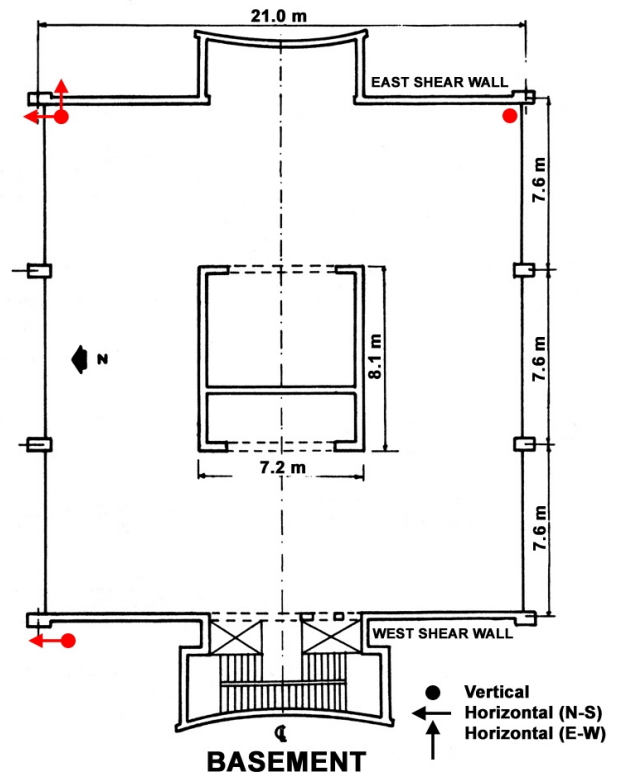
(a) North South Cross Section



(b) Foundation Plan View and North-South Cross Section



FLOORS 1-ROOF



BASEMENT

● Vertical  
 ◀ Horizontal (N-S)  
 ▲ Horizontal (E-W)

(c) Floor Plan and Instrumentation of Millikan Library, dense instrument array shown in red, station MIK (on 9th floor) shown in black. Shaker position (roof level) also shown.

Figure 2. Millikan Library Diagrams

has summarized some of the previous data on Millikan Library's behavior under forced and ambient vibrations in Appendix B. The evolution of the building behavior, including some dramatic shifts in the fundamental modes, is documented in Clinton et al. (2003) and is reproduced here in Table 1 and Figure 3. A drop of 21% and 12% for the E-W and N-S fundamental modes since construction is noted. The primary cause for these shifts appears to be a permanent loss of structural stiffness which occurs during strong ground motions, most noticeably the San Fernando (1979) and Whittier Narrows (1987) events. Small fluctuations in natural frequencies have also been noted which can depend on weather conditions at the time of testing (Bradford and Heaton, 2004), in particular, the E-W and torsional fundamental frequencies have increased by ~3% in the days following large rainfalls. The frequencies observed during ambient studies also differ from the frequencies observed during forced vibration tests (Clinton et al, 2003).

Event/Test	East - West				North - South			
	Nat Freq. Hz	%diff1	%diff2	mx accn cm/s <sup>2</sup>	Nat Freq. Hz	%diff1	%diff2	mx accn cm/s <sup>2</sup>
forced vibrations, 1967	1.45	-	-	-	1.90	-	-	-
<b>Lytle Creek, 1970 M5.3, Δ=57km</b>	1.30	10.3	10.3	<b>49</b>	1.88	1.1	1.1	<b>34</b>
<b>San Fernando, 1971 M6.6, Δ=31km</b>	1.0	31.0	31.0	<b>306</b>	1.64	13.7	13.7	<b>341</b>
forced vibrations, 1974	1.21	16.6	16.6	-	1.77	6.8	6.8	-
<b>Whittier Narrows, 1987 M6.1, Δ=19km</b>	1.00	31.0	17.4	<b>262</b>	1.33	30.0	24.9	<b>534</b>
forced vibrations, 1988	1.18	18.6	2.5	-	1.70	10.5	4.0	-
<b>Sierra Madre, 1991M5.8, Δ=18km</b>	0.92	36.6	22.0	<b>246</b>	1.39	26.8	18.2	<b>351</b>
forced vibrations, 1993	1.17	19.3	0.8	-	1.69	11.1	0.6	-
<b>Northridge, 1994 M6.7, Δ=34km</b>	0.94	35.2	19.7	<b>143</b>	1.33	30.0	21.3	<b>512</b>
forced vibrations, 1994	1.15	20.6	1.7	-	1.67	12.1	1.2	-
forced vibrations, 1995	1.15	20.6	0.0	-	1.68	11.6	-0.6	-
<b>Beverly Hills, 2001 M4.2, Δ=26km</b>	1.16	20.0	-0.9	<b>9.3</b>	1.68	11.6	0.0	<b>11.8</b>
forced vibrations, 2002 - Full Weights	1.11	23.4	3.5	<b>3.6</b>	1.64	13.7	2.4	<b>8.0</b>
- 1/2 weights	1.14	21.4	0.9	<b>1.9</b>	1.67	12.1	0.6	<b>4.1</b>
<b>Big Bear, 2003 M5.4, Δ=119km</b>	1.07	26.2	6.1	<b>14.2</b>	1.61	15.3	3.6	<b>22.6</b>

Table 1. History of Millikan Library Strong Motion Behavior - Fundamental Modes. "%diff1" is the difference between the recorded frequency and that obtained in the first forced vibration tests (Kuroiwa, 1967). "%diff2" is the difference between the recorded frequency and that obtained in the most recent forced vibration test prior to the event. (adapted from Clinton, (2003))



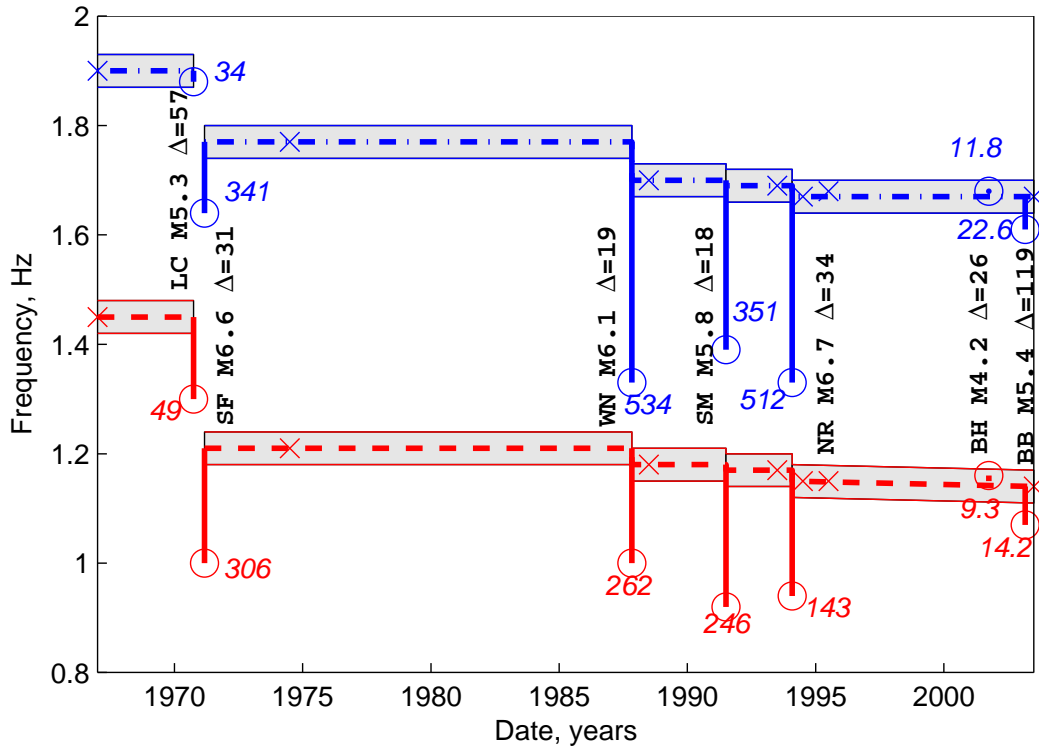


Figure 3. Graphical depiction of Table 1. Dashed lines represent the E-W natural frequencies and the dashed-dotted lines represent the N-S natural frequencies. Shaded area is the likely range of natural frequencies taking into consideration errors in measurement due to various factors - weight configuration in the shaker, weather conditions at the time of the test, and experimental error. Crosses indicate actual time forced test was made. Circles indicate natural frequency estimates from the strong motion record during earthquake events, and numbers in italics are peak acceleration recorded for the event ( $\text{cm/s}^2$ ). [Earthquake Abbreviations: LC: Lytle Creek, SF: San Fernando, WN: Whittier Narrows, SM: Santa Monica, NR: Northridge, BH: Beverly Hills, BB: Big Bear] (adapted from Clinton, (2003))

## 2.2 Millikan Library Shaker

A Kinematics model VG-1 synchronized vibration generator ("shaker") was installed on the roof of Millikan Library in 1972 (Figure 4). The shaker has two buckets that counter-rotate around a center spindle. These buckets can be loaded with different configurations of lead weights, and depending on the alignment of the buckets, the shaker can apply a sinusoidal force in any horizontal direction. The force ( $F_i$ ) applied by the shaker in each of its configurations can be expressed as:

$$\begin{aligned} A_1 &= 235.73 \text{ N} \cdot \text{sec}^2 \\ F_i &= A_i f^2 \sin(2\pi f t) \quad A_2 = 1518.67 \text{ N} \cdot \text{sec}^2 \quad (2.2.1) \\ A_3 &= 3575.89 \text{ N} \cdot \text{sec}^2 \end{aligned}$$

Frequency,  $f$ , is in Hz;  $A_i$  (a shaker constant) is in  $\text{N} \cdot \text{sec}^2$ ; and the resulting force,  $F_i$ , is in units of N. Table 2 lists the values of  $A_i$  and the limiting frequency for each weight configuration. For our test we used three shaker levels:  $A_3$ , full weights with the buckets loaded at 100% of capacity;  $A_2$ , an intermediate configuration with two large weights in each of the large weight sections of each bucket, corresponding to 42.5% of the mass of the full buckets; and  $A_1$ , empty buckets, which corresponds to a shake factor of 6.6% of the full weight configuration.

We can strongly excite the torsional modes through E-W shaking, as the shaker is located  $\sim 6.1$  meters to the South of the building's N-S line of symmetry (Figure 2c). The shaker is located  $\sim 0.3$  meters to the East of the building's E-W centerline, and therefore we do not expect shaking in the N-S direction to effectively excite the building in torsion.



Figure 4. Kinometrics VG-1 Synchronized Vibration Generator (Shaker). The counter-rotating buckets, shown empty, can be loaded with different configurations of lead weights. The shaker is located on the roof of Millikan Library, as shown in Figure 2.

		Small Weights				
		0	1	2	3	4
Large Weights	0	<b>235.73 [9.7]</b>	429.31 [7.2]	622.88 [6.0]	816.45 [5.2]	1010.03 [4.7]
	1	877.20 [5.0]	1070.77 [4.6]	1264.35 [4.2]	1457.92 [3.9]	1651.49 [3.7]
	2	<b>1518.67 [3.8]</b>	1712.24 [3.6]	1905.81 [3.4]	2099.39 [3.3]	2292.96 [3.1]
	3	2160.13 [3.2]	2353.71 [3.1]	2547.28 [3.0]	2740.85 [2.8]	2934.43 [2.8]
	4	2801.60 [2.8]	2995.17 [2.7]	3188.75 [2.6]	3382.32 [2.6]	<b>3575.89 [2.5]</b>

Table 2. Shaker constant,  $A_i$  ( $\text{N}\cdot\text{sec}^2$ ), and limiting frequencies [Hz] for different configurations of lead weights in the shaker. Bold type indicates the configurations used in these experiments.

## **2.3 Millikan Library Instrumentation**

In 1996 the United States Geological Survey (USGS) and the Caltech Department of Civil Engineering installed a permanent dense array of uni-axial strong-motion instruments (1g and 2g Kinematics FBA-11s) in the Millikan Library, with 36 channels recording on two 19-bit 18-channel Mt. Whitney digitizers. The instruments are distributed throughout the building, with three horizontal accelerometers located on each floor and three vertical instruments in the basement. This dense array is recorded by the Mt. Whitney digitizer system, providing local hard-drive storage of triggered events. In 2001 a 3-component Episensor together with a 24-bit Q980 data logger was installed on the 9th floor. Data from this sensor is continuously telemetered to the Southern California Seismic Network (SCSN) as station MIK. Figure 2c provides a schematic of the instrument locations.

### 3 FREQUENCY SWEEP

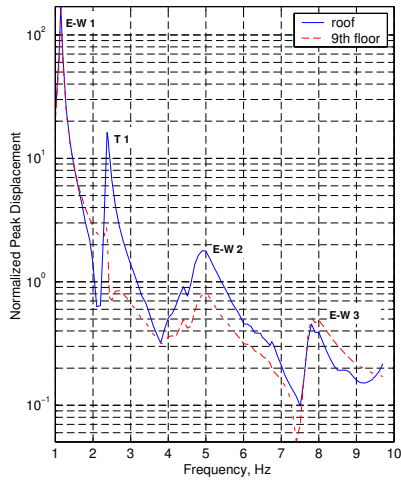
A frequency sweep of Millikan Library was performed on July 10, 2002. This test was designed to identify the natural frequencies and their damping; modeshapes would be determined with later detailed testing. The building response was recorded using the SCSN station MIK on the 9th floor, and a Mark Products L4C3D seismometer with a 16 bit Reftek recorder on the roof (provided by the Southern California Earthquake Center (SCEC) Portable Broadband Instrument Center located at U C Santa Barbara). We also used a Ranger seismometer with an oscilloscope at the roof level to provide an estimate of roof level response during our experiment.

We began with a N-S frequency sweep and the shaker set with empty buckets, starting near the frequency limit of the shaker at 9.7Hz. We held the frequency constant for approximately 60 seconds, to allow the building response to approach steady state, and then lowered the shaker frequency, in either .05Hz or .1Hz increments, again pausing for 60 seconds at each frequency. Once we reached 3.8Hz, we turned off the shaker, and loaded it with two large weights in each of the large weight compartments in each of the buckets (the intermediate 42.5% loading configuration). We then continued the frequency sweep from 3.7Hz to 1.5Hz. This procedure was repeated for the E-W direction — driving the empty shaker from 9.7Hz to 3.8Hz, then sweeping from 3.7Hz to 1Hz using the intermediate configuration.

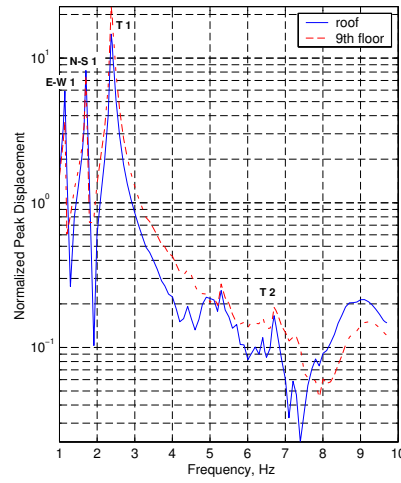
Figure 5 shows normalized peak displacement curves for the frequency sweeps. For each frequency, a representative section from the steady state portion of the data was selected, bandpass filtered (0.2Hz above and below each frequency, using a 2-pass 3-pole butterworth filter), and fit to a sine wave to estimate the exact frequency, amplitude, and phase. These sinusoidal amplitudes were then normalized by the applied shaker force for the particular frequency and weight combination (Equation 2.2.1).

Furthermore, damping was determined by applying the half-power (band-width) method (Meirovitch, 1986). We estimated the peak displacement frequency from a cubic interpolation of the normalized data,

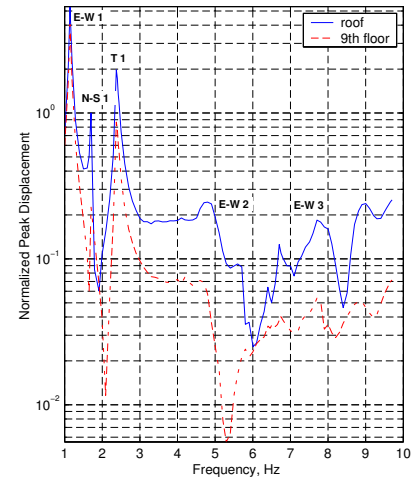
as our data sampling is somewhat sparse for a frequency/amplitude curve. As the higher modes have too much lower mode participation to determine the half-power points, damping was only determined for the fundamental modes. Damping is estimated to be 2.28%, 2.39% and 1.43% for the E-W, N-S and Torsional fundamental modes, respectively.



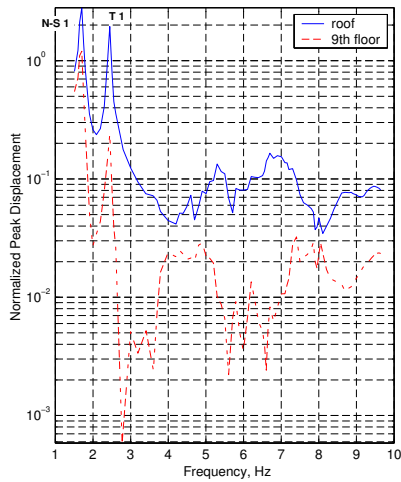
(a) East-West Response — East-West Excitation



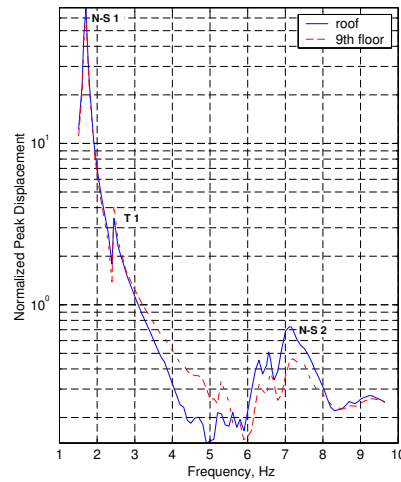
(b) North-South Response — East-West Excitation



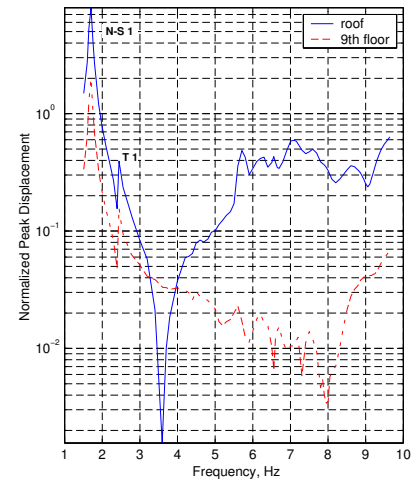
(c) Vertical Response — East-West Excitation



(d) East-West Response — North-South Excitation



(e) North-South Response — North-South Excitation



(f) Vertical Response — North-South Excitation

Figure 5. Lin-Log normalized peak displacement curves for the frequency sweep performed on July 10, 2002. Amplitudes for E-W and N-S shaking are normalized by the force factor corresponding to the weight configuration and frequency, as calculated in Equation 2.2.1. Roof response given by solid blue lines and station MIK (9th floor) response shown in dashed red lines.

## 4 MODESHAPE TESTING

We performed a forced excitation test of Millikan Library on August 18, 2002, recording data using the dense instrumentation network operated by the USGS and station MIK. We compare the behavior of the library with the behavior of uniform shear and bending beams (see Appendix A), but it is important to note that these are simple structural approximations which do not include the behavior of the foundation or the true structural system of the library.

Mode	Shake Direction/ Weight Configuration	Resonance Peak (Hz)	Normalized Roof Displacement [cm/N] x 10 <sup>-7</sup>	Percent Roof Displacement due to tilt and translation
Fundamental E-W	E-W / 100%	1.11	175(E-W)	3%
	E-W / 42.5%	1.14	180(E-W)	3%
Fundamental N-S	N-S / 100%	1.64	80(N-S)	30%
	N-S / 42.5%	1.67	80(N-S)	30%
Fundamental Torsion	E-W / 42.5%	2.38	25(N-S)	2% *
	N-S / 100%	2.35	5(N-S)	2% *
	N-S / 42.5%	2.38	5(N-S)	2% *
1 <sup>st</sup> E-W Overtone	E-W / 6.6%	4.93	2(E-W)	1%
1 <sup>st</sup> N-S Overtone	N-S / 6.6%	7.22	0.8(E-W)	-21%
1 <sup>st</sup> Torsion Overtone	E-W / 6.6%	6.57	0.4(E-W) / 0.15(N-S)	23% *
	N-S / 6.6%	6.70	0.5(N-S)	23% *
2 <sup>nd</sup> E-W Overtone	E-W / 6.6%	7.83	0.6(E-W)	0%

\*: % of rotation recorded at roof due to basement rotation

Table 3. Summary of Results for Modeshape Testing of August 28, 2002

### 4.1 Procedure and Data Reduction

We began the experiment with the shaker buckets fully loaded and set to excite the E-W direction. We excited the building at frequencies near the fundamental E-W and torsional modes, in frequency increments of .03-.05 Hz (again holding for 60s at each frequency to allow the building to approach steady-state response). With full buckets we then set the shaker to excite in the N-S direction to examine the fundamental N-S mode. We then repeated the excitation of the fundamental E-W, N-S and torsional



modes with the intermediate 42.5% weight configuration, to examine whether there is any shift in the natural frequencies depending on the exciting force. With empty shaker buckets, we excited the first and second E-W overtones, the first torsional overtone, and the first N-S overtone. Table 3 summarizes our testing procedure and results.

There are two parallel arrays of instruments in the N-S direction: one set located on the east side of the library, and the other on the west side of the library, as shown in Figure 2. In the E-W orientation there is one array, located on the west side of the building. The two N-S arrays are positioned towards the East and West edges of the building, far from the E-W centerline, while the E-W array on the west side of the building is located only 1m from the N-S centerline. Therefore, we expect to observe torsional response as strong, out of phase motion from the N-S arrays, with relatively small motion observed from the E-W array.

For each frequency, we selected a representative section from the the steady-state portion of the data, bandpassed the data (1/2 octave above and below each frequency using a 2-pass 2-pole butterworth filter) and integrated twice to obtain displacement values. We created resonance curves by fitting the displacement data to a sine wave to estimate frequency and amplitude, and then normalizing the response based on the applied force for each frequency and weight combination (Section 2.2). The mode shape snapshots in Figures 6 to 11 depict the behavior of the building at the point of maximum roof displacement for each frequency. Using the geometry of the basement and the position of the vertical basement sensors, we were able to estimate the rigid body rocking of the building and use it to correct our mode shapes. The horizontal basement sensors were used to correct for rigid building translation. Our mode shape figures present the raw results from all three instrument arrays, and the corrected results with basement translation and rocking removed.

For the torsional modes, in Figures 8 and 11, we present a snapshot of the displacement records, and also provide a snapshot in terms of rotation angle,  $\theta$ , at each floor. The rotation angle at each floor was

calculated by subtracting the western N-S array displacement values ( $D_2$ ) from the eastern N-S array displacement values ( $D_1$ ) and dividing by the E-W length ( $L_{E-W}$ ) between the arrays (Equation 4.1.1). For our rotation angle figures, we present the rotation angle at each floor, the basement rotation angle, and the rotation angle corrected for basement rotation.

$$\theta \approx \tan \theta = \frac{D_1 - D_2}{L_{E-W}} \quad (4.1.1)$$

Two of the instruments in the Eastern N-S array malfunctioned, on floors 2 and 8, and as a result we show a linearly interpolated value for those floors in our mode shape diagrams.

## 4.2 Fundamental Modes

### East-West Fundamental Mode

Figures 6a and 6b show the resonance curve obtained from forced E-W shaking with full weights and 42.5% weights respectively. Figures 6c and 6d present the respective mode shapes observed at the resonant frequencies for the different weight configurations. Shapes from all three sets of channels are shown on the same plot — the E-W response clearly dominates during E-W excitation. The observed mode shapes for different weight configurations are similar, but due to the non-linear force-response behavior of the building, the resonant frequency shifts from 1.11Hz with full weights to 1.14Hz with 42.5% weights. This shift in resonant frequency with respect to changing the applied force is small, and though obvious, is at the limit of the resolution of our survey.

Figures 6c and 6d show the mode shapes for both the raw displacements and the displacements corrected for translation and tilt. The mode shapes have a strong linear component, and closely resemble the theoretical mode shape for a bending beam, with the inclusion of the kink at the ground floor. See

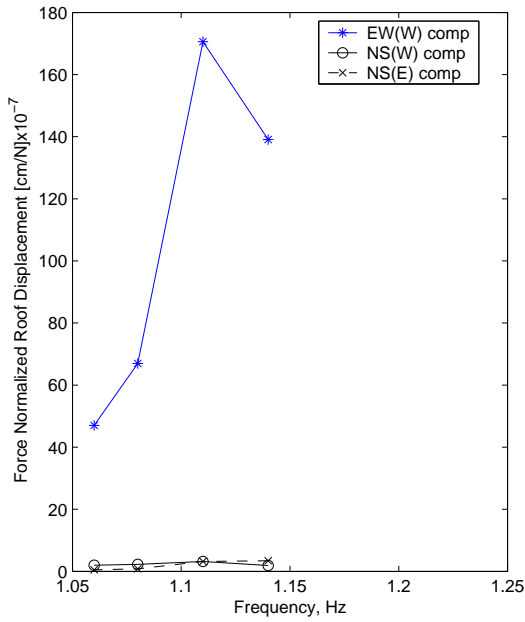
Appendix A for a brief summary and comparison of bending and shear beam behavior. Tilting and translation effects in this mode account for 3% of the roof displacement.

### **North-South Fundamental Mode**

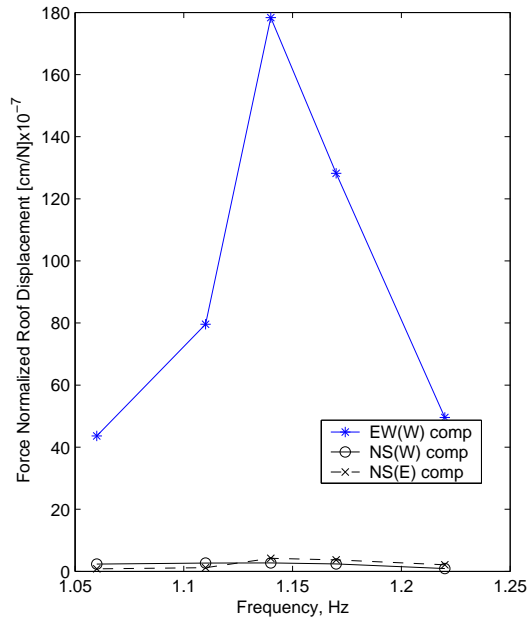
Figures 7a and 7d contain the resonance curves for N-S shaking with full weights and 42.5% weights, respectively. The fundamental N-S mode is also non-linear with respect to applied force, and we observe a resonant frequency shift from 1.64Hz for full weights to 1.67Hz with 42.5% weights. The mode shapes, Figure 7c and Figure 7d, are near identical, and show a more pronounced hinge behavior than the first E-W mode. When compared to the theoretical mode shapes of Appendix A, the observed shape most closely resembles theoretical bending beam behavior, differing near the ground floor due to the pronounced hinging behavior in this mode shape. We also observe that the two N-S arrays are exhibiting in-phase motion, and that the E-W response to N-S shaking is small, as expected. Foundation compliance becomes much more important for this mode, as we observe that  $\sim 25\%$  of the roof displacement is due to tilting of the library, and  $\sim 5\%$  is due to translation of the base of the library. Similar observations for the rigid-body rotation and translation of the building were made by Foutch et al. (1975).

### **Torsional Fundamental Mode**

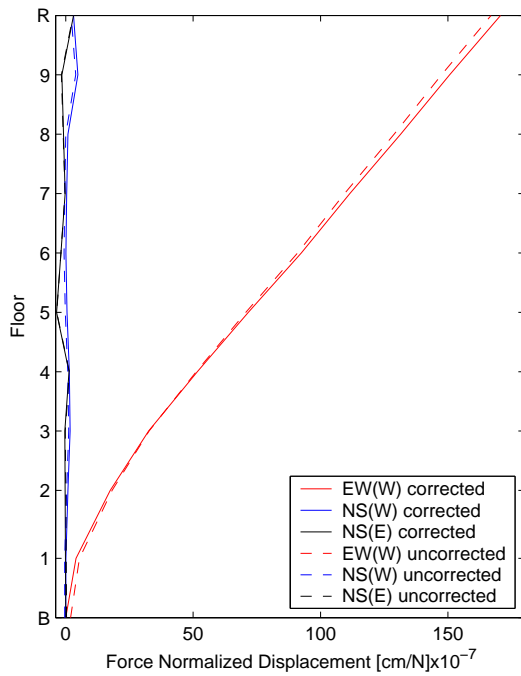
The fundamental torsional mode involves the twisting of the building and therefore has more complicated three-dimensional behavior. Due to the positioning of the instruments, a small amplitude response is observed from the accelerometers in the E-W array, while the two N-S arrays recorded a large amplitude out of phase response. Figure 8a shows the resonance curve for the fundamental torsional mode. Figure 8b gives the displacement records for the torsional mode shapes and Figure 8c shows the torsional mode shapes in terms of twist angle,  $\theta$  (as defined in Section 4.1), instead of displacement. In Figure 8b the two N-S arrays display the expected out of phase displacements, although some asymmetry is observed.



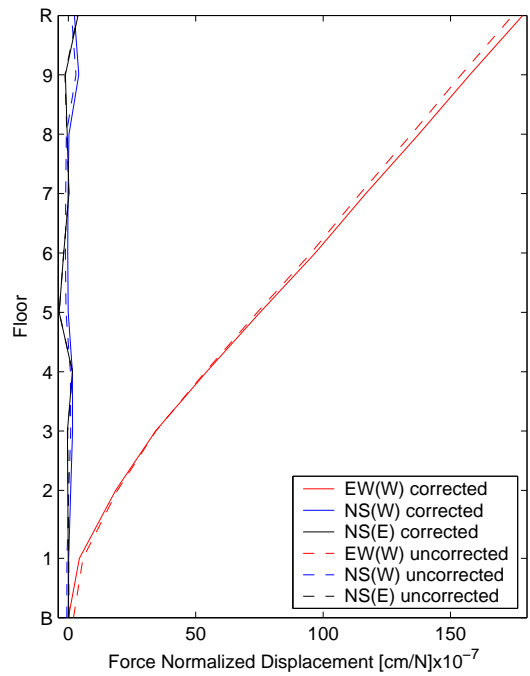
(a) Resonance curve for E-W Shaking, full weights



(b) Resonance curve for E-W Shaking, 42.5% weights

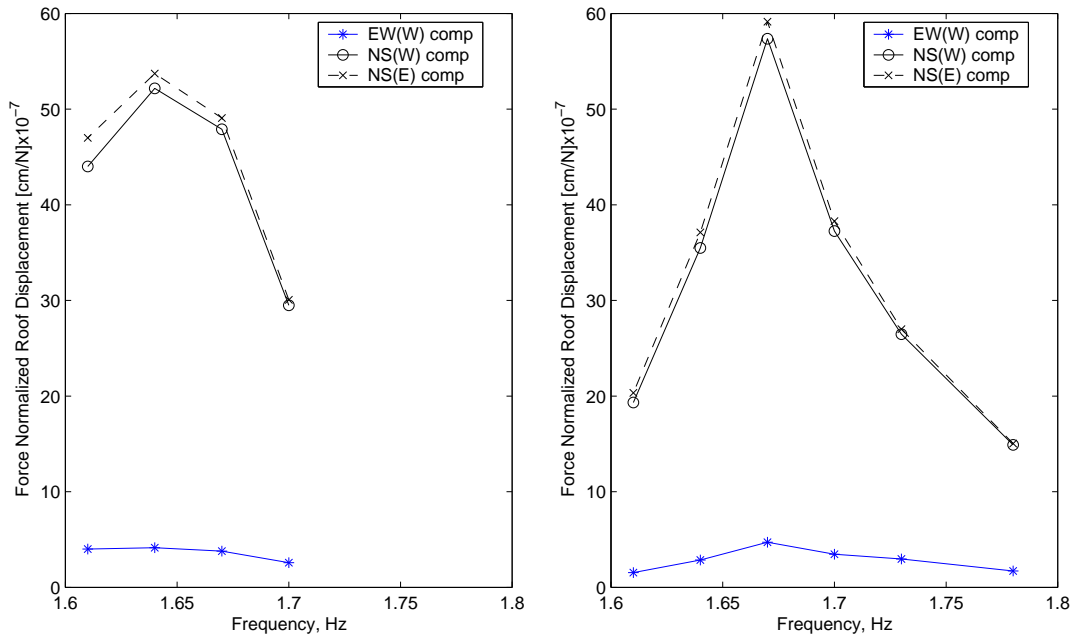


(c) Snapshot of building behavior at 1.11Hz, full weights, Force = 4,405.9N

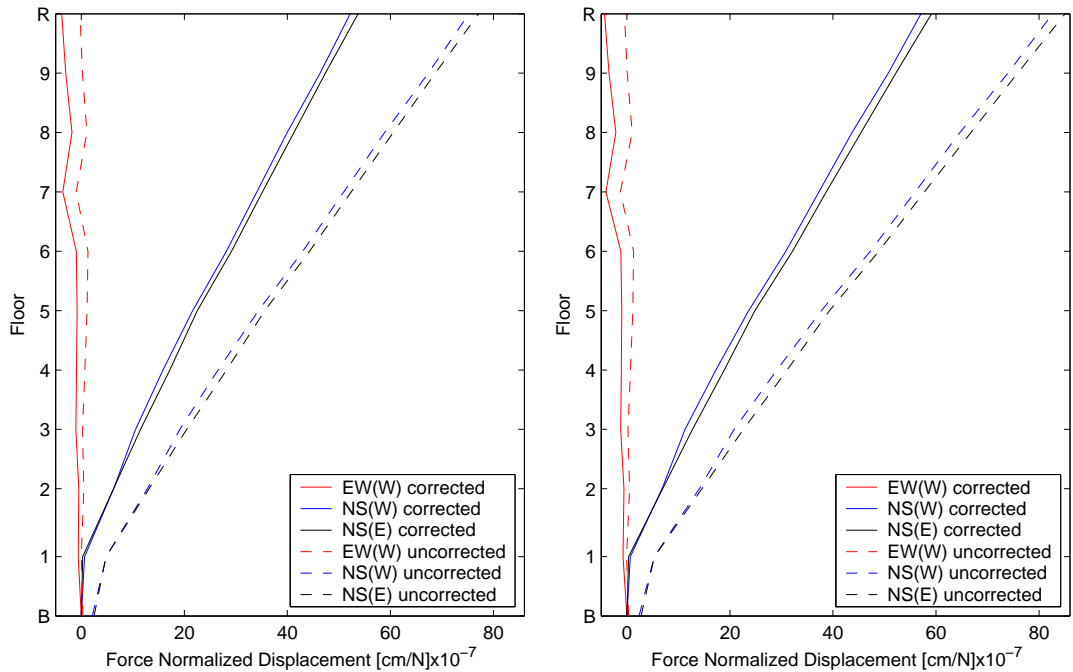


(d) Snapshot of building behavior at 1.14Hz, 42.5% weights, Force = 1,973.7N

Figure 6. Resonance curves and mode shapes for the E-W fundamental mode under two loading conditions. Mode shapes are shown corrected for rigid body motion and uncorrected. The mode shapes and resonance curves are shown for the east-west array located on the west side of the building, EW(W); the western north-south array, NS(W); and the eastern north-south array, NS(E). Force is calculated as in Equation 2.2.1, based on the frequency and loading configuration of the shaker.

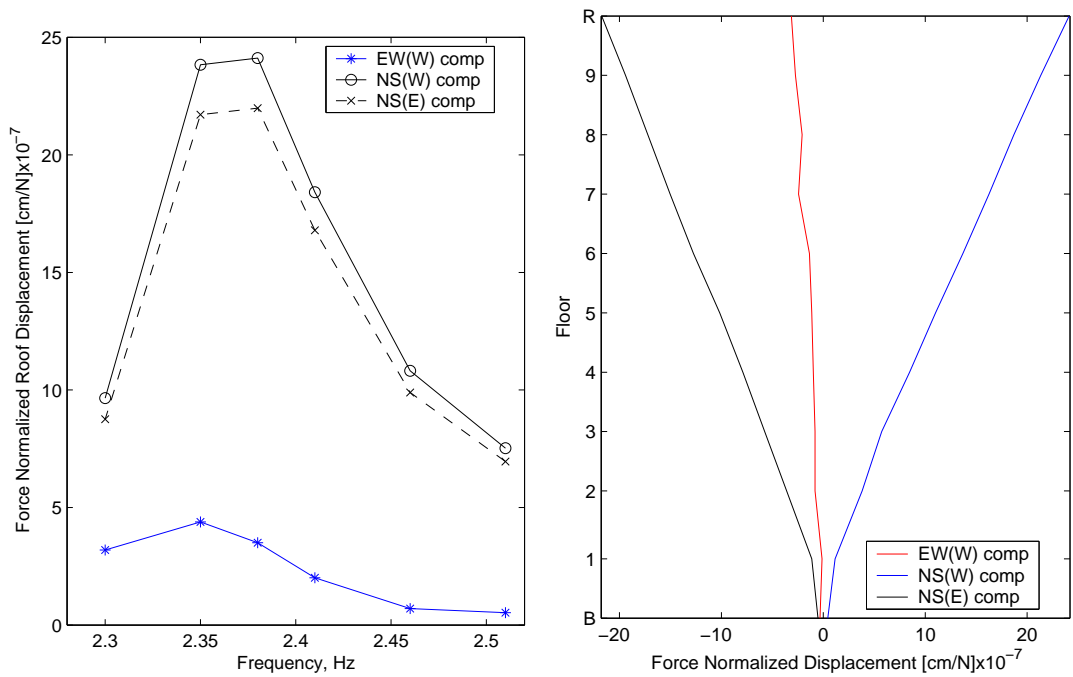


(a) Resonance curve for N-S Shaking, full weights (b) Resonance curve for N-S Shaking, 42.5% weights



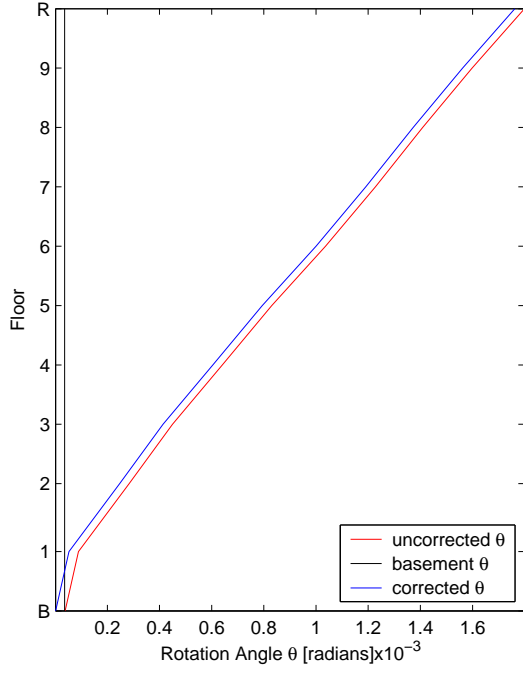
(c) Snapshot of building behavior at 1.64Hz, full weights, Force = 9,617.7N (d) Snapshot of building behavior at 1.67Hz, 42.5% weights, Force = 4,235.4N

Figure 7. Resonance curves and mode shapes for the N-S fundamental mode under two loading conditions. Mode shapes are shown corrected for rigid body motion and uncorrected. The mode shapes and resonance curves are shown for the east-west array, located on the west side of the building, EW(W); the western north-south array, NS(W); and the eastern north-south array, NS(E). Force is calculated as in Equation 2.2.1, based on the frequency and loading configuration of the shaker.



(a) Resonance curve for E-W Shaking, 42.5% weights

(b) Snapshot of building behavior at 2.38Hz, 42.5% weights, Force = 8,602.3N



(c) Snapshot of building behavior in terms of rotation angle  $\theta$ . Same configuration as in subfigure 8(b). The uncorrected snapshot is the rotation angle at each floor, calculated as in Equation 4.1.1. The corrected snapshot is the basement rotation angle subtracted from the rotation angle at each floor.

Figure 8. Resonance curves and mode shapes for the Torsional fundamental mode. Force is calculated as in Equation 2.2.1, based on the frequency and loading configuration of the shaker.

### **4.3 Higher Order Modes**

Prior to the installation of the dense instrument array, the higher order mode shapes were difficult to observe; determining the modeshapes and frequencies for these higher order modes was one of the primary goals of our suite of experiments.

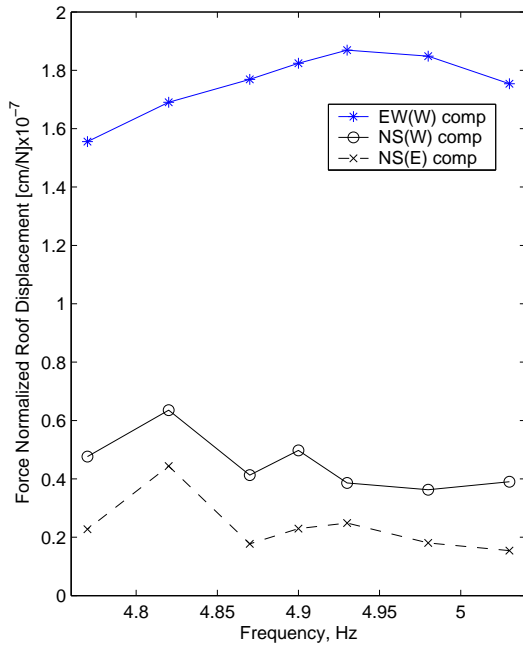
#### **Second and Third East-West Modes**

The first E-W overtone (second E-W mode) has a broad resonance peak, with a maximum response at 4.93Hz (Figure 9a). The mode shape, seen in Figure 9c, is typical of the second mode shape of a beam in bending (Appendix A). The ratio of the frequency of the second mode to the first mode is 4.32, much lower than the theoretical ratio for a bending beam of 6.26. For comparison, the theoretical ratio for a shear beam is 3.

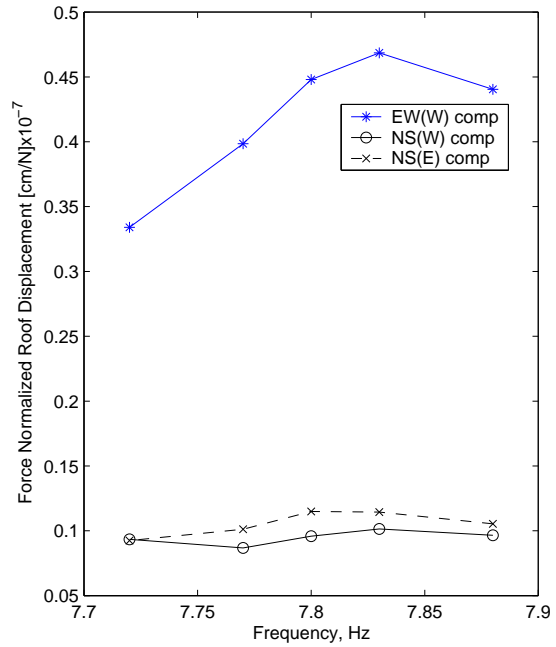
Also observed during our testing was the second E-W overtone (third E-W mode). Figure 9b shows a resonance peak with a maximum response at 7.83Hz. The mode shape for this frequency is presented in Figure 9d, and is typical of the second mode of a theoretical shear beam (Appendix A). The ratio of the frequency of the third mode to the second mode is 1.59, lower than the theoretical ratio for a bending beam of 2.80 and closer to the theoretical ratio for a shear beam of 1.67. The ratio of third mode to first mode frequencies for a bending beam is 17.55, the ratio for a shear beam is 5, and for our observed building behavior the ratio is 6.87.

#### **Second North-South Mode**

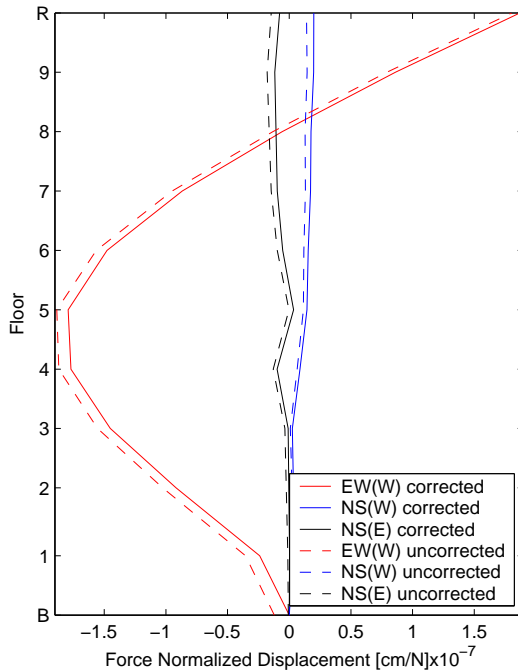
As can be seen in Figure 10a, the first N-S overtone (second N-S mode) also has a broad resonance peak. The resonance curves for the two N-S arrays did not have their peaks at the same frequency, so this test did not provide a single resonance peak. However, based on the frequency sweep of Section 3, and the shapes of the two resonance curves, we selected 7.22Hz as the modal frequency. The mode shape at this



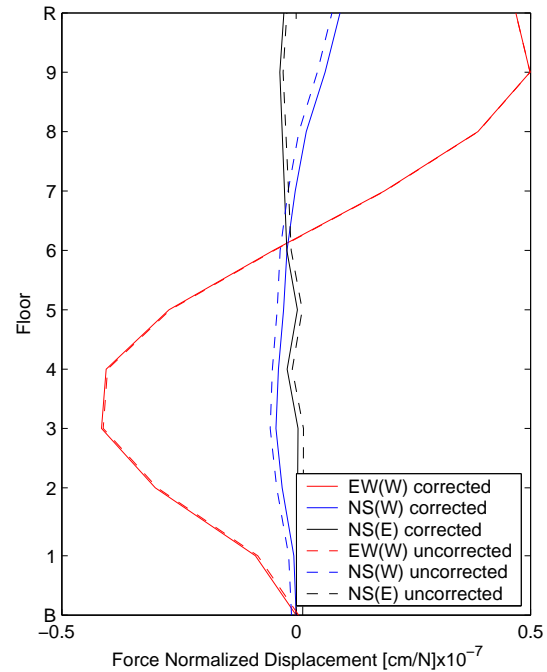
(a) Second E-W mode. Resonance curve for E-W Shaking, empty buckets



(b) Third E-W mode. Resonance curve for E-W shaking, empty buckets



(c) Second E-W mode. Snapshot of building behavior at 4.93Hz, empty buckets, Force = 6,166.9N



(d) Third E-W mode. Snapshot of building behavior at 7.83Hz, empty buckets, Force = 14,452.3N

Figure 9. Second and third E-W modes (first and second E-W overtones). Resonance curves and mode shapes. Mode shapes are shown corrected for rigid body motion and uncorrected. The mode shapes and resonance curves are shown for the east-west array, located on the west side of the building, EW(W); the western north-south array, NS(W); and the eastern north-south array, NS(E). Force is calculated as in Equation 2.2.1, based on the frequency and loading configuration of the shaker.



frequency, shown in Figure 10b, is qualitatively typical of a bending beam’s second mode, but we see that the two N-S arrays have very different amplitudes with zero crossings at different heights. For the N-S second mode, the eastern and western arrays should have similar shapes and amplitudes (cf. the first N-S mode, Figure 7), as the building is approximately symmetric. This implies that we did not excite the exact modal frequency, or that this mode has a more complicated three-dimensional response than the first N-S mode. The ratio of the frequency for the second mode (approximate) to the first mode is 4.32, which is close to the ratio of frequencies observed in E-W bending, and is also lower than the theoretical ratio for the first two modes of a bending beam.

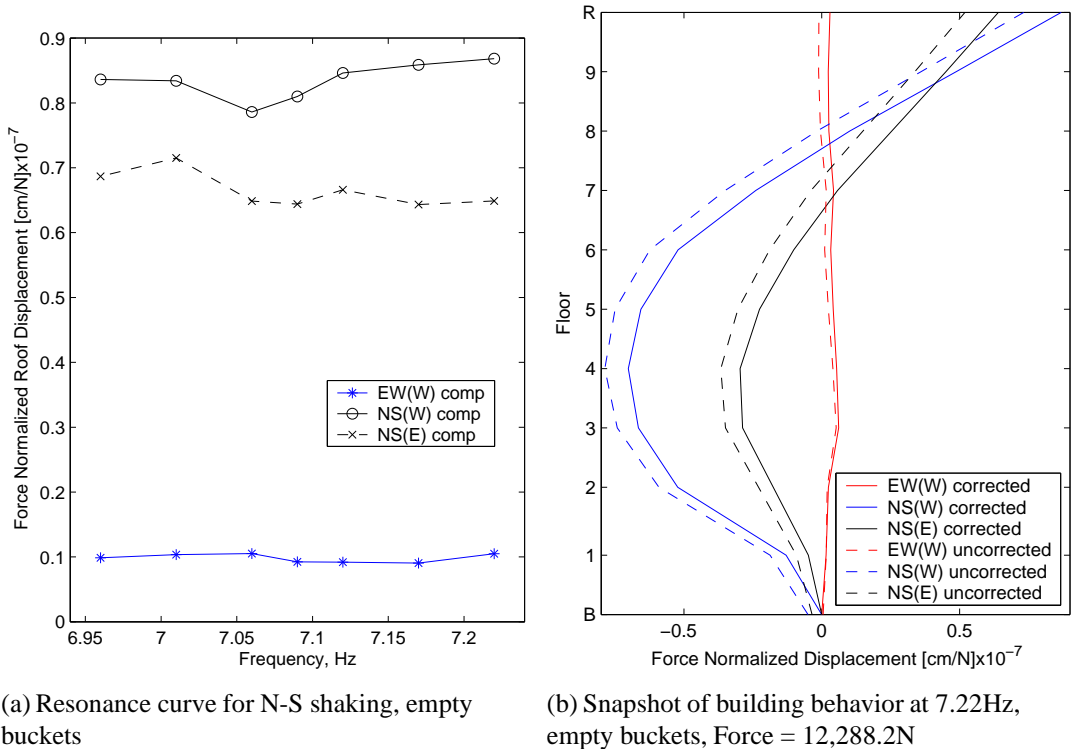
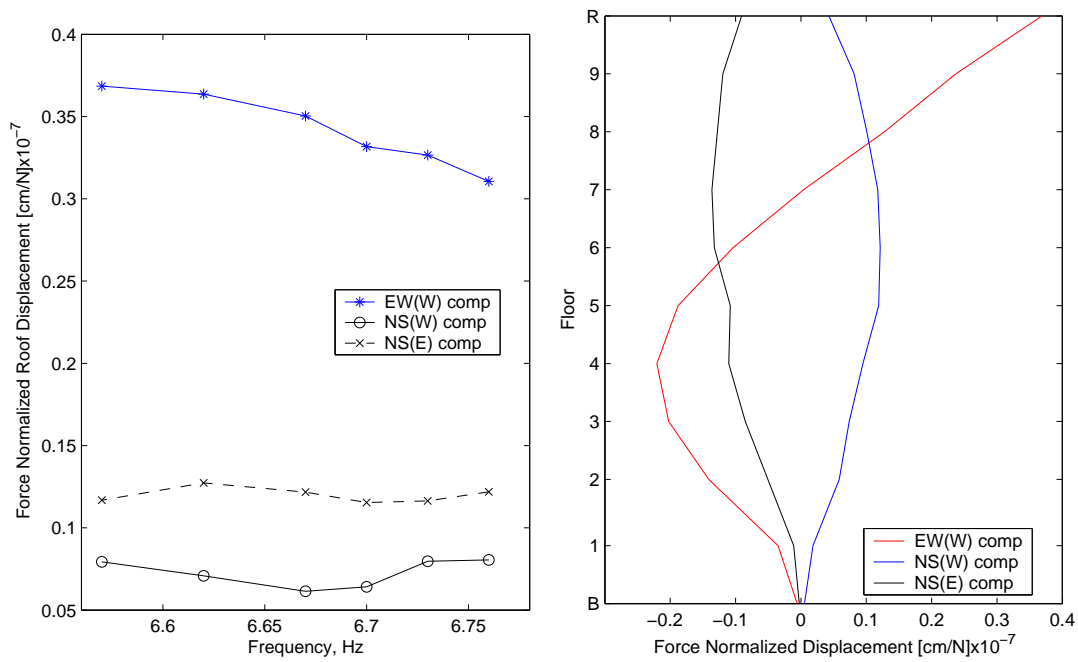


Figure 10. Resonance curves and mode shapes for the second NS mode (first NS overtone). Mode shapes are shown corrected for rigid body motion and uncorrected. The mode shapes and resonance curves are shown for the east-west array, located on the west side of the building, EW(W); the western north-south array, NS(W); and the eastern north-south array, NS(E). Force is calculated as in Equation 2.2.1, based on the frequency and loading configuration of the shaker.

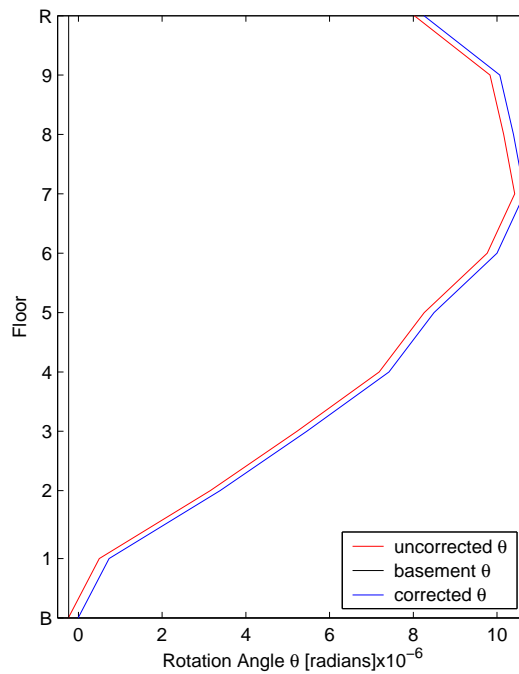
## Second Torsional Mode

The first torsional overtone was difficult to excite in the building, and difficult to observe. We excited the torsional mode using E-W excitation, and expected small torsional response on the E-W channels, and large out of phase response from the two N-S arrays. However, the observed response was dominated by E-W motion from the E-W shaking used to excite the system, which drove the building in a mode shape similar to that of the second E-W mode. We observed out of phase motion in the two N-S arrays, but the response of the N-S arrays was much smaller than the E-W response. Figure 11a shows the response curve for this mode, which is dominated by the E-W motion. Figure 11b shows the mode shapes, and Figure 11c shows the response in terms of twist angle,  $\theta$ , as defined in Section 4.1. As with the N-S overtone, the resonance curve did not clearly identify a modal frequency, but we chose 6.57Hz as the frequency of interest based on the shapes of the resonance curves and the results of the frequency sweep of Section 3.



(a) Resonance curve for E-W shaking, empty buckets

(b) Snapshot of building behavior at 6.57Hz, empty buckets, Force = 10,175.3N



(c) Snapshot of building behavior in terms of rotation angle  $\theta$ . Same configuration as in subfigure 11(b). The uncorrected snapshot is the rotation angle at each floor, calculated as in Equation 4.1.1. The corrected snapshot is the basement rotation angle subtracted from the rotation angle at each floor.

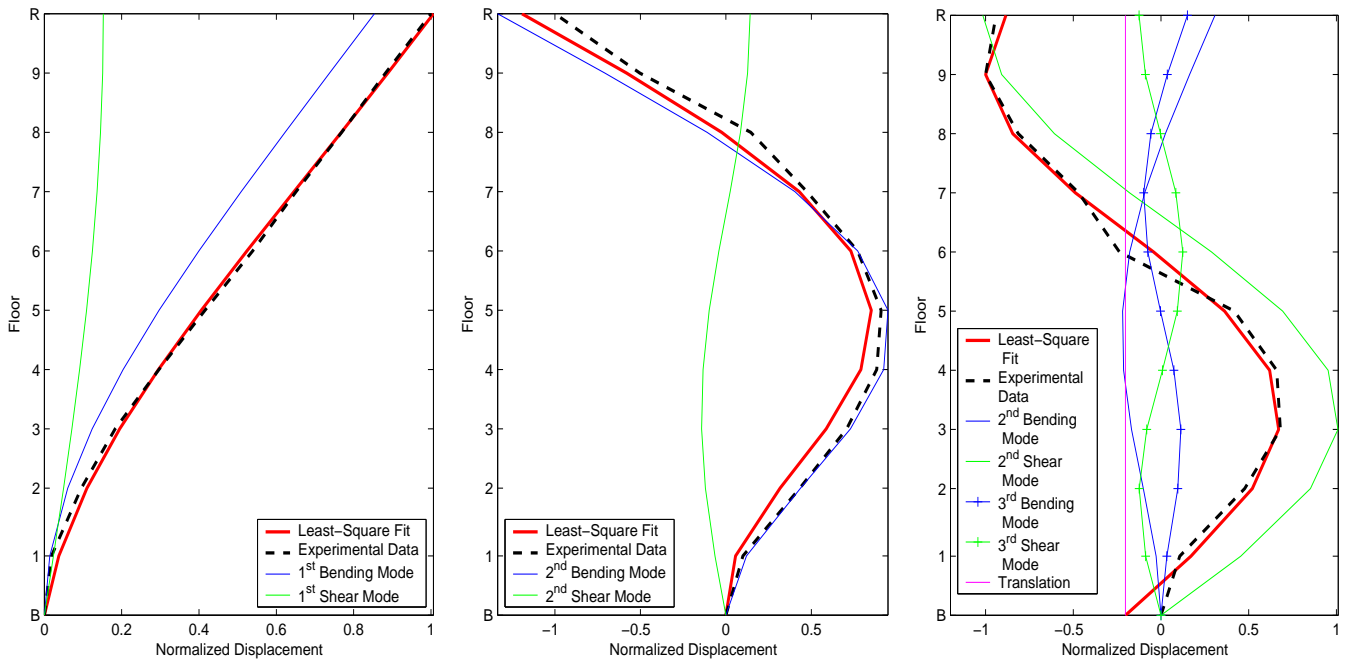
Figure 11. Resonance curves and mode shapes for the second Torsional mode (first Torsional overtone). Force is calculated as in Equation 2.2.1, based on the frequency and loading configuration of the shaker.

## 4.4 Modeshapes Summary

Table 4 contains a summary of the ratios of frequencies found for Millikan Library, along with theoretical results for bending and shear beams. Appendix A presents a summary of theoretical bending and shear beam behavior. To further analyze the data, the mode shapes were fit using theoretical bending and shear beam behavior by a modified least squares method. Figures 12 and 13 show the results of the least squares curve-fitting for the E-W and N-S modes respectively. The experimental data and best fit are shown, along with the theoretical mode shapes which are scaled according to their participation in the best fit curve. Both the fundamental E-W and N-S modes, Figures 12a and 13a, are dominated by the bending component, as are the second E-W and N-S modes, Figures 12b and 13b. The third E-W mode was not matched well using the third theoretical bending and shear modes; a fit including the second theoretical bending and shear modes is presented in Figure 12c, implying that the mode shape is best approximated by the second mode of a theoretical shear beam.

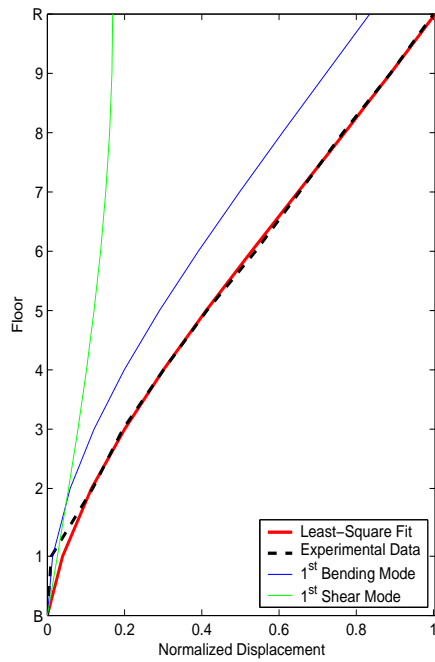
	Bending	Shear	Millikan E-W	Millikan N-S
$\omega_2/\omega_1$	6.26	3	4.32	4.32
$\omega_3/\omega_1$	17.55	5	6.87	N/A
$\omega_3/\omega_2$	2.8	1.67	1.57	N/A

Table 4. Ratio of frequencies for bending beam behavior, shear beam behavior, and the observed behavior of Millikan Library.

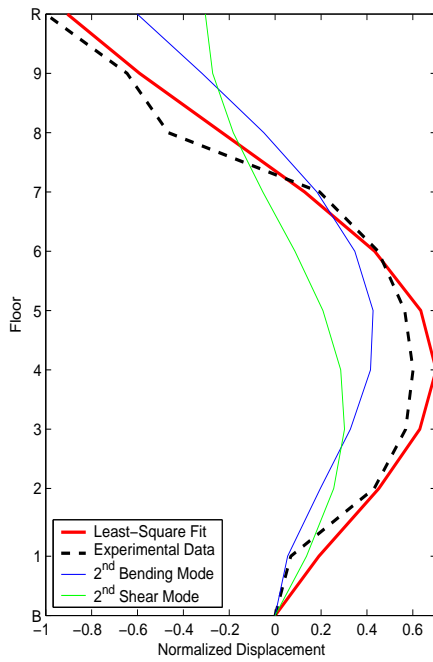


(a) Least square fit for fundamental E-W mode.  
 (b) Least square fit for second E-W mode (first E-W overtone).  
 (c) Least square fit for third E-W mode (second E-W overtone). Translational term included in curve-fitting to accommodate large kink at ground level.

Figure 12. Least squares curve fitting for E-W modes. Tilt and translation removed.



(a) Least square fit for fundamental N-S mode.



(b) Least square fit for second E-W mode (first E-W overtone).

Figure 13. Least squares curve fitting for N-S modes. Tilt and translation removed.

## REFERENCES

- Beck, J. L. and E. Chan (1995). Comparison of the response of millikan library to san fernando and whittier narrows earthquakes.
- Beck, J. L., B. S. May, and D. C. Polidori (3-5 August 1994). Determination of modal parameters from ambient vibration data for structural health monitoring. In *First World Conference on Structural Control*, Los Angeles, California, USA.
- Blandford, R., V. R. McLamore, and J. Aunon (1968). Analysis of millikan library from ambient vibrations. Technical report, Earth Teledyne Co.
- Bradford, S. C. and T. H. Heaton (2004). Weather patterns and wandering frequencies in a structure. *in preparation*.
- Chopra, A. K. (1995). *Dynamics of Structures - Theory and Applications to Earthquake Engineering*, Chapter 11, pp. 409–414, 514–515. Prentice Hall.
- Clinton, J. F. (2004). *Modern Digital Seismology - Instrumentation and Small Amplitude Studies for the Engineering World*. Ph.D. thesis, California Institute of Technology. In Preparation.
- Clinton, J. F., S. C. Bradford, T. H. Heaton, and J. Favela (2003). The observed drifting of the natural frequencies in a structure. *in preparation*.
- Favela, J. (2003). *Energy Radiation and Curious Characteristics of Millikan Library*. Ph.D. thesis, California Institute of Technology. In Preparation.
- Foutch, D. A. (1976). *A Study of the Vibrational Characteristics of Two Multistorey Buildings*. Ph.D. thesis, California Institute of Technology, Earthquake Engineering Research Laboratory, Pasadena, California.
- Foutch, D. A., J. E. Luco, M. D. Trifunac, and F. E. Udawadia (1975). Full scale, three dimensional tests of structural deformation during forced excitation of a nine-storey reinforced concrete building. In *Proceedings, U.S. National Conference on Earthquake Engineering*, Ann Arbor, Michigan, pp. 206–215.
- Iemura, H. and P. C. Jennings (1973). Hysteretic response of a nine-storey reinforced concrete building during the san fernando earthquake. Technical report, Earthquake Engineering Research Laboratory, California Institute of Technology.
- Jennings, P. C. and J. H. Kuroiwa (1968). Vibration and soil-structure interaction tests of a nine-storey reinforced concrete building. *Bulletin of the Seismological Society of America* 58(3), 891–916.
- Kuroiwa, J. H. (1967). *Vibration Test of a Multistorey Building*. Ph.D. thesis, California Institute of Technology, Earthquake Engineering Research Laboratory, Pasadena, California.
- Luco, J., M. Trifunac, and H. Wong (1987). On the apparent change in dynamic behavior of a 9- story reinforced-concrete building. *BULLETIN OF THE SEISMOLOGICAL SOCIETY OF AMERICA* 77(6), 1961–1983.
- Luco, J. E., W. H. L., and T. M. D. (1986, September). Soil-structure interaction effects on forced vibration tests. Technical Report Report 86-05, University of Southern California, Department of Civil Engineering, Los Angeles, California.
- McVerry, G. H. (1980). *Frequency Domain Identification of Structural Models from Earthquake Records*. Ph.D. thesis, California Institute of Technology.
- Meirovitch, L. (1986). *Elements of Vibration Analysis*. McGraw-Hill, Inc.
- Teledyne-Geotech-West (1972). Post earthquake vibration measurements millikan library. Technical report, Teledyne Geotech West, Monrovia, California.
- Trifunac, M. D. (1972). Comparisons between ambient and forced vibration experiments. *Earthquake Engineering and Structural Dynamics* 1, 133–150.
- Udawadia, F. E. and P. Z. Marmarelis (1976). The identification of building structural systems: I. the linear case. *BULLETIN OF THE SEISMOLOGICAL SOCIETY OF AMERICA* 66(1), 125–151.
- Udawadia, F. E. and M. D. Trifunac (1973). Ambient vibration tests of a full-scale structures. In *Proceedings, Fifth World Conference on Earthquake Engineering*, Rome.
- Udawadia, F. E. and M. D. Trifunac (1974). Time and amplitude dependent response of structures. *Int. J. Earthquake Engineering and Structural Dynamics* 2, 359–378.

Department of Civil Engineering  
Division of Engineering and Applied Science  
California Institute of Technology  
Pasadena, CA 91125  
S C Bradford: case@ecf.caltech.edu



## A THEORETICAL BEAM BEHAVIOR

*Adapted from Meirovitch, (1986).*

The mode shape and frequencies for a cantilevered (fixed-free) bending beam are found by solving the differential equation:

$$\frac{\partial^4 X(z)}{\partial z^4} - \beta^4 X(z) = 0 \quad \beta^4 = \frac{\omega^2 m}{EI}$$

m = Mass/Unit Length, E = Young's Modulus, I = Moment of Inertia

With the following boundary conditions:

$$X(0) = 0 \qquad \frac{\partial X(z)}{\partial z} \Big|_{x=0} = 0 \qquad \text{At the fixed end}$$

$$\frac{\partial^2 X(z)}{\partial z^2} \Big|_{x=L} = 0 \qquad \frac{\partial^3 X(z)}{\partial z^3} \Big|_{x=L} = 0 \qquad \text{At the free end}$$

This leads to the characteristic equation:

$$\cos(\beta L) \cosh(\beta L) = -1$$

Which can be solved analytically to give the following values for the first three modes:

$$\text{Mode 1 : } \beta_1 L = 1.875$$

$$\text{Mode 2 : } \beta_2 L = 4.694$$

$$\text{Mode 3 : } \beta_3 L = 7.855$$

$$\text{with } \omega_i = \beta_i^2 \sqrt{\frac{EI}{mL^4}}$$

The mode shapes are given by:

$$X_n(z) = C_1 \left[ (\sin \beta_n z - \sinh \beta_n z) + \frac{(\cos \beta_n L + \cosh \beta_n L)}{(\sin \beta_n L - \sinh \beta_n L)} (\cos \beta_n z - \cosh \beta_n z) \right]$$

The first three modes are plotted in Figure A.1.

Theoretical shear beam behavior is as follows, with the deformed shape being portions of a sine curve:

$$X_n(z) = C_1 \left[ \left( \sin \frac{(2n-1)\pi}{2} z \right) \right] \quad n = 1, 2, 3 \dots$$

The first three modes are plotted in Figure A.2.

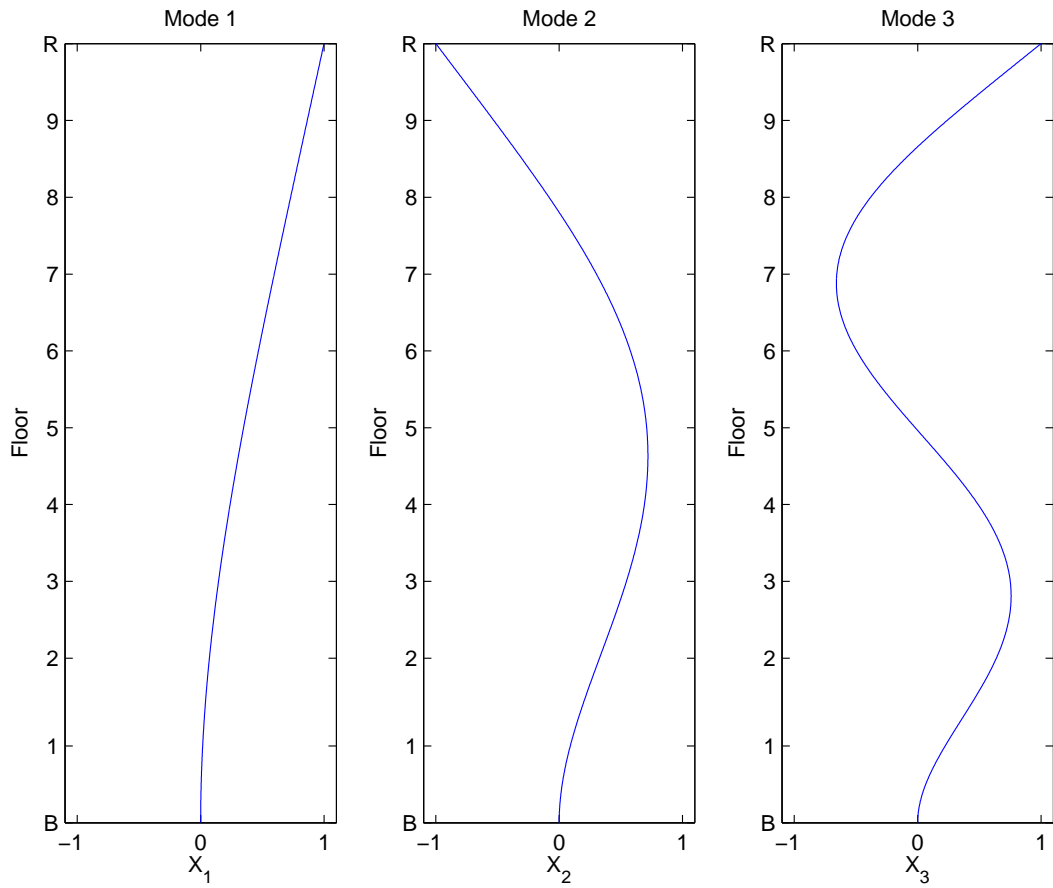


Figure A.1. From left to right, theoretical mode shapes for the fundamental mode (1st mode) and the first two overtones (2nd and 3rd modes) for a cantilevered bending beam. Mode shapes  $X_n$  are normalized such that the maximum displacement is equal to 1.

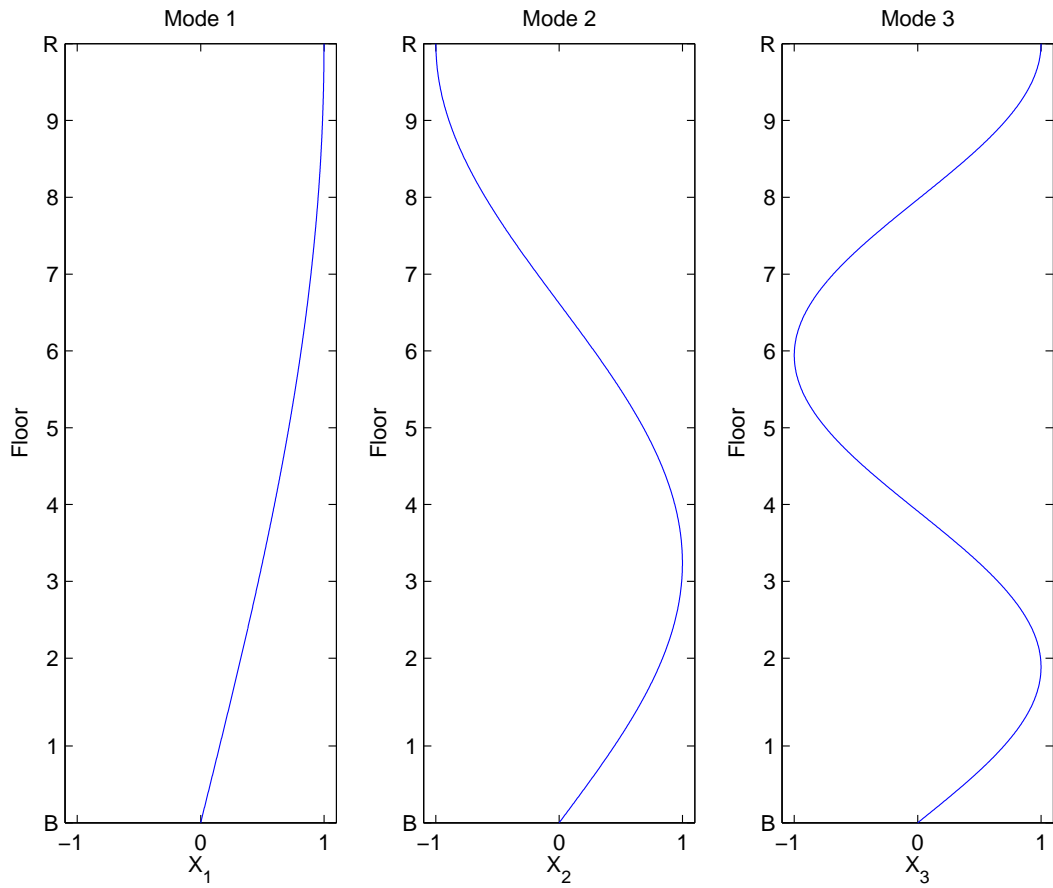


Figure A.2. From left to right, theoretical mode shapes for the fundamental mode (1st mode) and the first two overtones (2nd and 3rd modes) for a cantilevered shear beam. Mode shapes  $X_n$  are normalized such that the maximum displacement is equal to 1.

## **B HISTORICAL SUMMARY OF MILLIKAN LIBRARY STUDIES**

*Adapted from Clinton (2004).*

Tables B.1 and B.2 provide a summary of various studies into the frequencies and damping of Millikan Library. Table B.3 contains the references used to compile Tables B.1 and B.2. These studies include ambient and forced vibration testing, as well as data recorded from earthquake ground motions.

Test	East - West		North - South		Torsional		Remark
	$f_0$ [ $\zeta_0$ ]	$f_1$ [ $\zeta_1$ ]	$f_0$ [ $\zeta_0$ ]	$f_1$ [ $\zeta_1$ ]	$f_0$ [ $\zeta_0$ ]	$f_1$ [ $\zeta_1$ ]	
1966-1967 <sup>1</sup>	1.46-1.51 [0.7-1.7]	6.2	1.89-1.98 [1.2-1.8]	-	2.84-2.90 [0.9-1.6]	-	A,F,M
Mar 1967 <sup>2</sup>	1.49 [1.5]	6.1	1.91 [1.6]	-	2.88	-	A
Apr 1968 <sup>3</sup>	1.45	6.1	1.89	9.18	2.87	9.62	A
Jul 1969 <sup>4</sup>	1.45	5.90	1.89	9.10	-	-	A
Sep 12 1970 <sup>5</sup>	1.30-1.50	-	1.90-2.10	-	-	-	E (LC)
Sep 12 1970 <sup>6</sup>	1.30	-	1.88	-	-	-	E (LC)
~ M6.7 February 9 1971 San Fernando Earthquake (SF) @ 44km ~							
Feb 9 1971 <sup>5</sup>	1.00-1.50	-	1.50-1.90	-	-	-	E (SF)
Feb 9 1971 <sup>7</sup>	0.82-1.43 [1.0-13.0]	-	-	-	-	-	E (SF)
Feb 9 1971 <sup>8</sup>	1.02-1.11 [3.5-5.5]	-	-	-	-	-	E (SF)
Feb 9 1971 <sup>9</sup>	1.03 [0.07]	4.98 [0.06]	1.61 [0.06]	7.81 [0.06]	-	-	E (SF)
Feb 9 1971 <sup>10</sup>	1.02 [0.06]	4.93 [0.05]	1.61 [0.06]	7.82 [0.05]	-	-	E (SF)
Feb 9 1971 <sup>6</sup>	1.00	-	1.64	-	-	-	E (SF)
Feb 1971 <sup>11</sup>	1.27 [2.5]	5.35 [0.9]	1.8 [3]	9.02 [0.2]	2.65 [2]	9.65 [0.5]	A
Feb 1971 <sup>4</sup>	1.30	-	-	-	-	-	A
Dec 1972 <sup>4</sup>	1.37	-	1.77	-	-	-	M
Apr 1973 <sup>12</sup>	1.28 [1.3]	-	-	-	-	-	A
1974 <sup>13</sup>	1.21	-	1.76	-	-	-	F
Jul 1975 <sup>14</sup>	1.21 [1.8]	-	1.79 [1.8]	-	-	-	F
May 1976 <sup>9</sup>	1.27	-	1.85	-	2.65	-	A
~ M6.1 October 1 1987 Whittier Narrows Earthquake (WN) @ 19km ~							
Oct 1 1987 <sup>10</sup>	0.932 [0.04]	4.17 [0.08]	1.30 [0.06]	6.64 [0.18]	-	-	E (WN)
Oct 1 1987 <sup>6</sup>	1.00	-	1.33	-	-	-	E (WN)
Oct 4 1987 <sup>10</sup>	0.98	-	1.43	-	-	-	E(WN M5.3)
Oct 16 1987 <sup>10</sup>	1.20	-	1.69	-	-	-	E(WN M2.8)
May 1988 <sup>11</sup>	1.18	-	1.70	-	-	-	F
~ M5.8 June 28 1991 Sierra Madre Earthquake (SM) @ 18km ~							
June 28 1991 <sup>6</sup>	0.92	-	1.39	-	-	-	E (SM)
May 1993 <sup>15</sup>	1.17	-	1.69	-	2.44	-	F
~ M6.7 January 17 1994 Northridge Earthquake (N) @ 34km ~							
Jan 17 1994 <sup>6</sup>	0.94	-	1.33	-	-	-	E (N)
Aug 2002 <sup>18</sup>	1.14 [2.28]	4.93	1.67 [2.39]	7.22	2.38 [1.43]	6.57	F

Table B.1. Summary of Millikan Library Modal Frequency and Damping Analysis Experiments 1967-1994.  $f_0$  and  $f_1$  are the fundamental frequency and the first overtone, in Hz.  $\zeta_0$  and  $\zeta_1$  are the corresponding damping ratios, in %. References are found in Table B.3. A: Ambient, M: Man Excited, F: Forced Vibration, E: Earthquake Motions [LC: Lytle Creek Earthquake]

Test	East - West		North - South		Torsional		Remark
	$f_0$ [ $\zeta_0$ ]	$f_1$ [ $\zeta_1$ ]	$f_0$ [ $\zeta_0$ ]	$f_1$ [ $\zeta_1$ ]	$f_0$ [ $\zeta_0$ ]	$f_1$ [ $\zeta_1$ ]	
1966-1967 <sup>1</sup>	1.46-1.51	6.2	1.89-1.98	-	2.84-2.90	-	A,F,M
	[0.7-1.7]		[1.2-1.8]		[0.9-1.6]		
Mar 1967 <sup>2</sup>	1.49 [1.5]	6.1	1.91 [1.6]	-	2.88	-	A
~ M6.7 February 9 1971 San Fernando Earthquake (SF) @ 44km ~							
Feb 9 1971 <sup>6</sup>	1.00	-	1.64	-	-	-	E (SF)
May 1976 <sup>9</sup>	1.27	-	1.85	-	2.65	-	A
~ M6.1 October 1 1987 Whittier Narrows Earthquake (WN) @ 19km ~							
Oct 1 1987 <sup>10</sup>	0.932 [0.04]	4.17 [0.08]	1.30 [0.06]	6.64 [0.18]	-	-	E (WN)
Oct 1 1987 <sup>6</sup>	1.00	-	1.33	-	-	-	E (WN)
Oct 4 1987 <sup>10</sup>	0.98	-	1.43	-	-	-	E(WN M5.3)
Oct 16 1987 <sup>10</sup>	1.20	-	1.69	-	-	-	E(WN M2.8)
May 1988 <sup>11</sup>	1.18	-	1.70	-	-	-	F
~ M5.8 June 28 1991 Sierra Madre Earthquake (SM) @ 18km ~							
June 28 1991 <sup>6</sup>	0.92	-	1.39	-	-	-	E (SM)
May 1993 <sup>15</sup>	1.17	-	1.69	-	2.44	-	F
~ M6.7 January 17 1994 Northridge Earthquake (N) @ 34km ~							
Jan 17 1994 <sup>6</sup>	0.94	-	1.33	-	-	-	E (N)
Jan 19 1994 <sup>15</sup>	1.13	-	1.65	-	2.39	-	F
Jan 20 1994 <sup>15</sup>	1.13	4.40-4.90	1.65	8.22-8.24	2.39	-	A
	[1.2-2.1]	[1.0]	[0.7-1.5]	[0.2-0.3]	[0.3-0.5]		F
May 1994 <sup>16</sup>	1.15 [1.38]	-	1.67 [1.46]	-	2.4 [1.18]	-	F
May 1995 <sup>16</sup>	1.15 [1.44]	-	1.68 [1.25]	-	2.42 [1.15]	-	F
May 1998 <sup>16</sup>	1.17 [1.4]	-	1.70 [1.3]	-	2.46	-	F
May 1998 <sup>16</sup>	-	-	1.68	1.5	-	-	M
May 2000 <sup>16</sup>	1.15 [3]	-	1.66 [3]	-	2.41 [2.5]	-	F
May 2000 <sup>16</sup>	-	-	1.72 [0.8]	-	-	-	A
May 2001 <sup>16</sup>	1.11 [3.25]	-	1.63 [3.69]	-	2.31 [2.9]	-	F
May 2001 <sup>16</sup>	-	-	1.71 [1.2]	-	-	-	M
Dec 2001 <sup>17</sup>	1.12 [1.63]	-	1.63 [1.65]	-	2.34	-	F
Sep 9 2001 <sup>6</sup>	1.16	-	1.68	-	-	-	E (BH M4.2)
Aug 2002 <sup>18</sup>	1.14 [2.28]	4.93	1.67 [2.39]	7.22	2.38 [1.43]	6.57	F
Feb 22 2003 <sup>6</sup>	1.07	-	1.61	-	-	-	E (BB M5.4)

Table B.2. Summary of Millikan Library Modal Frequency and Damping Analysis Experiments 1987-2003.  $f_0$  and  $f_1$  are the fundamental frequency and the first overtone, in Hz.  $\zeta_0$  and  $\zeta_1$  are the corresponding damping ratios, in %. References are found in Table B.3. A: Ambient, M: Man Excited, F: Forced Vibration, E: Earthquake Motions [BH: Beverly Hills Earthquake, BB: Big Bear Earthquake]

<b>Footnote #</b>	<b>Reference</b>	<b>Remarks</b>
1	Kuroiwa (1967)	<i>forced, ambient, man excitations</i> — <i>during and immediately after construction, Library not full</i>
2	Blandford et al. (1968)	<i>ambient</i>
3	Jennings and Kuroiwa (1968)	<i>ambient</i>
4	Udwadia and Trifunac (1973)	<i>ambient</i>
5	Udwadia and Trifunac (1974)	<i>Lyle Creek, San Fernando</i> — <i>based on transfer functions</i>
6	Clinton et al. (2003)	<i>Earthquakes</i> — <i>estimated from strong motion records</i>
7	Iemura and Jennings (1973)	<i>San Fernando</i>
8	Udwadia and Marmarelis (1976)	<i>San Fernando</i> — <i>based on linear model</i>
9	McVerry (1980)	<i>SanFernando; ambient</i>
10	Beck and Chan (1995)	<i>SanFernando, Whittier MODEID</i>
11	Teledyne-Geotech-West (1972)	<i>ambient - 1mth after San Fernando</i> — <i>Also Vertical <math>f_0 = 3 - 4\text{Hz}</math>, high <math>\zeta</math>.</i>
12	Udwadia and Marmarelis (1976)	<i>San Fernando</i>
13	Foutch et al. (1975)	<i>forced</i>
14	Luco et al. (1987)	<i>forced</i>
15	Beck et al. (1994)	<i>forced, ambient</i> — <i>Also Jan 20 Ambient test: EW3 at 7.83Hz</i>
16	CE180 Caltech - various students	<i>forced</i>
17	Favela, personal communication	<i>forced</i>
18	This report, Bradford et al. (2004)	<i>forced</i> — <i>Also EW3 at 7.83Hz</i>

Table B.3. References which correspond to footnote numbers in Tables B.1 and B.2.